DMD Fast Forward. Published on October 20, 2021 as DOI: 10.1124/dmd.121.000605
This article has not been copyedited and formatted. The final version may differ from this version.

Simultaneous evaluation of membrane permeability and UDP-glucuronosyltransferase-mediated metabolism of food-derived compounds using human induced pluripotent stem cell-derived small intestinal epithelial cells

Takashi Kitaguchi [a, *], Taisei Mizota [a], Mina Ito [a], Katsutoshi Ohno [a], Kazuhiro Kobayashi [a], Isamu Ogawa [b], Shimeng Qiu [b], Takahiro Iwao [b], Nobumitsu Hanioka [c], Mitsuru Tanaka [a], and Tamihide Matsunaga [b]

[a] Global Food Safety Institute, Nissin Foods Holdings Co., Ltd., 2100 Tobuki-machi, Hachioji, Tokyo, 192-0001, Japan

[b] Department of Clinical Pharmacy, Graduate School of Pharmaceutical Sciences, Nagoya City University, 3-1 Tanabe-dori, Mizuho-ku, Nagoya, 467-8603, Japan

[c] Department of Health Pharmacy, Yokohama University of Pharmacy, 601 Matano-cho, Totsuka-ku, Yokohama, 245-0066, Japan

DMD Fast Forward. Published on October 20, 2021 as DOI: 10.1124/dmd.121.000605
This article has not been copyedited and formatted. The final version may differ from this version.

Running Title: Membrane permeability and UGT metabolism in hiPSC-SIECs

*** Corresponding author: Takashi Kitaguchi**

Global Food Safety Institute, Nissin Foods Holdings Co., Ltd., 2100 Tobuki-machi, Hachioji, Tokyo, 192-0001, Japan.

Telephone: +81-42-696-7836

E-mail address: takashi.kitaguchi@nissin.com

Number of text pages: 19

Number of tables: 4

Number of figures: 2

Number of references: 33

Number of words in Abstract: 170

Number of words in Introduction: 750

Number of words in Discussion: 1643

Abbreviations: CYP, cytochrome P450; DMEM, Dulbecco's modified Eagle's medium; DMSO, dimethyl sulfoxide; F_a or F_aF_g, intestinal availability; FBS, fetal bovine serum; HBSS, Hanks' balanced salt solution; hiPSC-SIEC, human induced pluripotent stem

DMD Fast Forward. Published on October 20, 2021 as DOI: 10.1124/dmd.121.000605
This article has not been copyedited and formatted. The final version may differ from this version.

cell-derived small intestinal epithelial cell; hPEC, human primary enterocyte; MeIQx, 2-amino-3,8-dimethylimidazo[4,5-f]quinoxaline; MES, 2-(*N*-morpholino)ethanesulfonic acid; NEAA, nonessential amino acids solution; P_{app}, apparent permeability coefficient; RT-PCR, reverse transcription polymerase chain reaction; UGT, UDP-glucuronosyltransferase; UPLC-MS/MS, ultraperformance liquid chromatography-tandem mass spectrometry

DMD Fast Forward. Published on October 20, 2021 as DOI: 10.1124/dmd.121.000605
This article has not been copyedited and formatted. The final version may differ from this version.

Abstract

Pharmacokinetic prediction after oral ingestion is important for quantitative risk assessment of food-derived compounds. To evaluate the utility of human intestinal absorption prediction, we compared the membrane permeability and metabolic activities of human induced pluripotent stem cell-derived small intestinal epithelial cells (hiPSC-SIECs) with Caco-2 cells or human primary enterocytes (hPECs). We found that membrane permeability in hiPSC-SIECs had better predictivity than that in Caco-2 cells against 21 drugs with known human intestinal availability (r = 0.830 and 0.401, respectively). Membrane permeability in hiPSC-SIECs was only 0.019–0.25-fold as compared with that in Caco-2 cells for 7 in 15 food-derived compounds, primarily those which were reported to undergo glucuronidation metabolism. The metabolic rates of the glucuronide conjugate were similar or higher in hiPSC-SIECs as compared with hPECs, while lower in Caco-2 cells. Expression levels of UDP-glucuronosyltransferase (UGT) isoform mRNA in hiPSC-SIECs were similar or higher as compared with hPECs. Therefore, hiPSC-SIECs could be a useful tool for predicting human intestinal absorption, in order to simultaneously evaluate membrane permeability and UGT-mediated metabolism.

DMD Fast Forward. Published on October 20, 2021 as DOI: 10.1124/dmd.121.000605
This article has not been copyedited and formatted. The final version may differ from this version.

Significance Statement

Gastrointestinal absorption is an important step for predicting the internal exposure of food-derived compounds. This research revealed that human induced pluripotent stem cell-derived small intestinal cells (hiPSC-SIECs) had better predictivity of intestinal availability than Caco-2 cells; furthermore, the metabolic rates of UGT substrates of hiPSC-SIECs were closer those of human primary enterocytes than those of Caco-2 cells. Therefore, hiPSC-SIECs could be a useful tool for predicting human intestinal absorption to simultaneously evaluate membrane permeability and UGT-mediated metabolism.

DMD Fast Forward. Published on October 20, 2021 as DOI: 10.1124/dmd.121.000605
This article has not been copyedited and formatted. The final version may differ from this version.

Introduction

Foods consist of a wide variety of compounds from the food itself, the environment, and also those generated during processing or storage, some of which possess functionality in the living body or have potential for harm (Gibis, 2016; Luca et al., 2020; Thompson and Darwish, 2019). Animal experiments are often used for human risk assessment to comprehensively understand the toxic mechanisms and pharmacokinetics of such compounds, but there are ethical issues and poor predictivity issues for different species (Punt et al., 2017). Well-controlled clinical trials are very limited for food-derived compounds, and are particularly limited to those that have concern for human health risks. In order to quantitatively assess whether a food-derived compound exerts effects *in vivo*, it is important to understand pharmacokinetics after oral ingestion, which can address the internal exposure levels and cellular toxic concentration of the compounds. Alternatives to animal experiments and clinical trials that can directly and quantitatively predict human internal exposure after oral ingestion are required as risk assessment tools.

To predict the internal exposure of food-derived compounds, an initial and important step is gastrointestinal absorption after oral ingestion. The gastrointestinal tract works as a functional barrier made of cells, incorporating nutrients, detoxifying and excreting xenobiotics, and possessing immune function (Shimizu, 2011). Human colon adenocarcinoma-derived Caco-2 cells are widely used to predict the intestinal absorption

DMD Fast Forward. Published on October 20, 2021 as DOI: 10.1124/dmd.121.000605
This article has not been copyedited and formatted. The final version may differ from this version.

(Larregieu and Benet, 2013; Vancamelbeke and Vermeire, 2017). Caco-2 cells cultured on a cell culture insert for about 3 weeks form a monolayer membrane and show similar morphological features to human intestinal epithelial cells, such as intercellular connections and microvilli formation, as well as cellular functions such as efflux transporter P-glycoprotein or breast cancer-resistance protein expression on the apical side. However, membrane permeability assays using Caco-2 cells have some limitations. First, permeability of compounds via the paracellular route in Caco-2 cells is very low, since the tight junction is strong compared with human small intestinal cells (Takenaka et al., 2016). Second, metabolism of compounds differs from human primary enterocytes (hPECs) because the expression levels and balances of metabolic enzymes such as cytochrome P450s (CYPs) and UDP-glucuronosyltransferases (UGTs) differ from those in human small intestinal epithelial cells (Zhang et al., 2011). UGT is one of the most important enzymes for intestinal absorption of food-derived compounds, and extensively metabolizes some of these compounds in the intestine and liver before they enter systemic circulation (Wu et al., 2011). Therefore, there is a long way to go to replace animal experiments with alternative *in vitro* methods to quantitatively predict the health risks of the compounds. Previously, predictions using parallel artificial membrane permeability assays and metabolic stability assays with human intestinal microsomes were combined with *in vitro*-*in vivo* extrapolation techniques (Nishimuta et al., 2011). However, this technique required two separate

DMD Fast Forward. Published on October 20, 2021 as DOI: 10.1124/dmd.121.000605
This article has not been copyedited and formatted. The final version may differ from this version.

experiments, and might not predict active and paracellular transports. More recently, new cells and methods, such as human small intestinal epithelial cells differentiated from adult intestinal stem cells and Ussing chambers with freshly isolated human jejunum using residual intestinal tissue after human surgery, have been reported to improve predictivity of human intestinal absorption (Michiba et al., 2021; Takenaka et al., 2016); however, these human-derived biomaterials have availability issues.

In recent years, human induced pluripotent stem cell-derived small intestinal epithelial cells (hiPSC-SIECs) have been developed and are commercially available from several vendors. hiPSC-SIECs have been reported to express various functional drug-metabolizing enzymes such as CYP3A4, and transporters comparable to those in human intestinal epithelial cells (Kabeya et al., 2020; Negoro et al., 2018). Moreover, differentiated hiPSC-SIECs that are easy to use can be obtained from cell vendors, and the intellectual property rights are included in these products for researchers. In addition, hiPSC-SIECs can form a monolayer on cell culture inserts, which cannot be formed by cryopreserved human primary small intestinal cells due to the limited period of viability after thawing. Therefore, the application of hiPSC-SIECs in membrane permeability assays is expected to improve the predictivity of oral availability *in vitro* by evaluating intracellular metabolism and transporter functions simultaneously. Although several studies have characterized hiPSC-SIECs (Kabeya et al., 2020; Negoro et al., 2018; Yoshida et al.,

2021), to our knowledge, reports on their application for membrane permeability assays in combination with metabolic characterization of UGTs for hiPSC-SIEC metabolism of food-derived compounds is limited. In this study, we compared the membrane permeability of hiPSC-SIECs and intestinal metabolic activity, especially by UGTs, with Caco-2 cells and human primary enterocytes (hPECs) in order to evaluate their utility for estimating the oral absorption of food-derived compounds for quantitative human risk assessment.

DMD Fast Forward. Published on October 20, 2021 as DOI: 10.1124/dmd.121.000605
This article has not been copyedited and formatted. The final version may differ from this version.

Materials and Methods

Cells and reagents

hiPSC-SIECs were purchased from Fujifilm Corporation (F-hiSIEC^{TM}, Tokyo, Japan), which included seeding and maintenance medium. Pre-plated Caco-2 cells were purchased from ReadyCell (CacoReady^{TM} Plate, Barcelona, Spain), and hPECs were purchased from In Vitro ADMET Laboratories (Columbia, MD). Dulbecco's modified Eagle's medium (DMEM), penicillin–streptomycin solution, nonessential amino acids solution (NEAA), and fetal bovine serum (FBS) were purchased from Thermo Fischer Scientific (Waltham, MA, USA). Hanks' balanced salt solution (HBSS) and dimethyl sulfoxide (DMSO) were purchased from Fujifilm Wako Pure Chemical Industries (Osaka, Japan).

The drugs, food-derived compounds, and metabolites listed below were dissolved in DMSO and stored at −20℃ until use. Carbamazepine, verapamil, warfarin, antipyrine, cephalexin, metoprolol, propranolol, hydrochlorothiazide, cimetidine, atenolol, pravastatin, methotrexate, curcumin, epicatechin, epigallocatechin, epigallocatechin gallate, bisphenol A, 2-amino-3,8-dimethylimidazo[4,5-f]quinoxaline (MeIQx), and 7-hydroxycoumarin were purchased from Fujifilm Wako Pure Chemical Industries. Piroxicam, acebutolol, sulpiride, acrylamide, fenitrothion, and β-estradiol were purchased from Sigma-Aldrich (St. Louis, MO, USA). Ribavirin, metformin, enalapril, ranitidine, bisphenol S, picloram, and

DMD Fast Forward. Published on October 20, 2021 as DOI: 10.1124/dmd.121.000605
This article has not been copyedited and formatted. The final version may differ from this version.

raloxifene were purchased from Tokyo Chemical Industry (Tokyo, Japan). Terbutaline was purchased from LKT Laboratories (St. Paul, MN, USA). Daidzein and genistein were purchased from LC Laboratories (Woburn, MA, USA). Quercetin was purchased from Nacalai Tesque (Kyoto, Japan). 7-Hydroxycoumarin glucuronide, 7-hydroxycoumarin sulfate, daidzein 4'-glucuronide, and daidzein 7-glucuronide were purchased from SantaCruz Biotechnology (Dallas, TX, USA). Raloxifene 4'-glucuronide and raloxifene 6-glucuronide, genistein 4'-glucuronide, and bisphenol A sulfate were purchased from Toronto Research Chemicals (Ontario, Canada). Genistein 7-glucuronide was purchased from Extrasynthese (Lyon France). Estradiol 3-glucuronide and estradiol 17-glucuronide were purchased from Cayman Chemical (Ann Arbor, MI, USA).

TB Green Premix Ex Taq (Tli RNaseH Plus) was purchased from Takara Bio (Shiga, Japan) and specific primer pairs were synthetized in FASMAC (Kanagawa, Japan). Matrigel was purchased from Corning (Corning, NY, USA). Cryopreserved enterocyte recovery medium and hepatocyte/enterocyte incubation medium were purchased from In Vitro ADMET Laboratories.

Cell culture

hiPSC-SIECs were thawed and seeded at a density of 1.0×10^5 cells/well on Matrigel-coated 24-well cell culture inserts (Merck Millipore, Burlington, MA, USA), and

DMD Fast Forward. Published on October 20, 2021 as DOI: 10.1124/dmd.121.000605
This article has not been copyedited and formatted. The final version may differ from this version.

then maintained for 9–13 days until use according to the manufacturer's instruction. Caco-2 cells were shipped on day 18 after seeding on 24-well cell culture inserts and maintained with DMEM supplemented with 1% NEAA, 10% FBS, and 50 U/mL penicillin/streptomycin for an additional 3–7 days according to the suppliers' instruction manual. hPECs were thawed according to the manufacturer's instructions and immediately used after plating. Transepithelial electronic resistance (TEER) values were measured with Millicell ERS-2 (Merck Millipore) just before the membrane permeability assays.

Membrane permeability assay

hiPSC-SIECs or Caco-2 cells were washed 3 times with apical transport buffer (HBSS containing 10 mM MES (Fujifilm Wako) and 4.5 g/L glucose, pH 6.5) and in basal transport buffer (HBSS containing 10 mM HEPES (Thermo Fischer Scientific) and 4.5 g/L glucose, pH 7.4) chambers, and incubated at 37°C for at least 30 min. Membrane transport assays were performed at 37°C for 30, 60, and 90 min after replenishing the apical chambers with transport buffer containing each substrate at a final concentration of 10 μM. The solution was collected from the basal chambers at 30 min intervals and diluted with an equal volume of acetonitrile, then stored at −20°C. Unreacted substrates and/or metabolites were measured using ultraperformance liquid chromatography-tandem mass spectrometry (UPLC-MS/MS). Intestinal availability (F_a or F_aF_g) data for humans were acquired from

DMD Fast Forward. Published on October 20, 2021 as DOI: 10.1124/dmd.121.000605
This article has not been copyedited and formatted. The final version may differ from this version.

publicly available data and detailed information is shown in Supplemental Table 1.

Metabolic rate measurement

hiPSC-SIECs or Caco-2 cells were cultured in 24-well cell culture inserts as described above, washed 3 times with transport buffer, and incubated for 30 min in a 5% CO_2 incubator. hPECs were thawed in cryopreserved enterocyte recovery medium and seeded with serum-free enterocyte incubation medium at a density of 1.5×10^5 cells/well on a flat-bottomed 96-well plate according to the manufacturer's instruction and incubated for 30 minutes in a 5% CO_2 incubator. These cells were exposed to UGT substrates at a concentration of 10 μM for 2 h. Finally, apical and basal buffers were obtained and diluted with equal volumes of acetonitrile and centrifuged at 10,000 g at 4°C for 5 min and supernatants were stored at −20°C until UPLC-MS/MS quantification.

mRNA expression levels

Real-time reverse transcription polymerase chain reaction (RT-PCR) was conducted according to previously published methods, with minor modifications (Ohno and Nakajin, 2009). Total RNA for hiPSC-SIECs, Caco-2 cells, and hPECs was extracted with RNeasy Plus Mini kit and RNase free DNase (Qiagen, Hilden, Germany). Reverse transcription was carried out using high-capacity RNA-to-cDNA kits (Thermo Fischer Scientific) according

DMD Fast Forward. Published on October 20, 2021 as DOI: 10.1124/dmd.121.000605
This article has not been copyedited and formatted. The final version may differ from this version.

to the manufacturer's recommendations, using 5 ng of total RNA as the template. Quantification of mRNA expression levels for human UGT isoforms was performed using the ViiA 7 system (Applied Biosystems, Foster City, CA, USA) in a total reaction volume of 20 μL/well, which consisted of 0.5 μM of each of the specific primer pairs (Table 1) and 2 μL of cDNA solution. PCR amplification consisted of an initial 30-sec denaturation step at 95°C, followed by 40 cycles of denaturation at 95°C for 5 s, and annealing and extension at 60°C for 30 s. Specificity of the PCR amplification was confirmed via analysis of the melting curve.

Data analysis

Apparent permeability coefficients (P_{app}) were calculated as follows:

$$P_{app} = dQ/dt \times [1/ (A \times C_0)]$$

where dQ/dt, A, and C_0 represent the amount of permeated compound per unit of time, the surface area of the transport membrane, and the initial compound concentration in the donor chamber, respectively. The relationship between apical-to-basal P_{app} and F_a or F_aF_g was calculated in accordance with previous reports (Takenaka et al., 2016 and Amidon et al., 1988).:

$$F_a \text{ or } F_aF_g = e^{-Psf \times Papp}$$

where P_{sf} is the scaling factor. Nonlinear regression was used for curve fitting with JMP

DMD Fast Forward. Published on October 20, 2021 as DOI: 10.1124/dmd.121.000605
This article has not been copyedited and formatted. The final version may differ from this version.

version 15 (SAS Institute, Cary, NC, USA). Relative gene expression data was analyzed using the $2^{-\Delta\Delta Ct}$ method (Livak and Schmittgen, 2001).

DMD Fast Forward. Published on October 20, 2021 as DOI: 10.1124/dmd.121.000605
This article has not been copyedited and formatted. The final version may differ from this version.

Results

Relationships between the P_{app} and F_a or F_aF_g using 21-known drugs

The TEER values of monolayers of hiPSC-SIECs and Caco-2 cells were 882 ± 258 (n = 42) and 1348 ± 377 (n = 63) Ω·cm^2, respectively. The relationships between P_{app} and F_a or F_aF_g for the 21 drugs investigated in hiPSC-SIECs and Caco-2 cells are shown (Fig. 1A–B). hiPSC-SIECs had a better correlation between P_{app} and F_a or F_aF_g (r = 0.830) than Caco-2 cells (r = 0.401). The estimated P_{sf} values of hiPSC-SIECs and Caco-2 cells were 3.38 ± 0.447 and 2.98 ± 0.815 × 10^6 s/cm, respectively.

Comparisons of P_{app} across food-derived compounds

Membrane permeabilities were compared between fifteen food-derived compounds in hiPSC-SIECs and Caco-2 cells (Table 2). The P_{app} values of daidzein, genistein, quercetin, curcumin, bisphenol A, bisphenol S, and MeIQx in hiPSC-SIECs were lower than those in Caco-2 cells. These compounds were reported to undergo glucuronidation, and the P_{app} values of hiPSC-SIECs ranged from 0.019 (curcumin) to 0.25-fold (bisphenol S) compared to those of Caco-2 cells. The P_{app} values of caffeic acid and gallic acid in hiPSC-SIECs were higher than those in Caco-2 cells. The P_{app} values of epicatechin, epigallocatechin, epigallocatechin gallate, acrylamide, fenitrothion, and picloram were within 0.71–1.3-fold between hiPSC-SIECs and Caco-2 cells.

DMD Fast Forward. Published on October 20, 2021 as DOI: 10.1124/dmd.121.000605
This article has not been copyedited and formatted. The final version may differ from this version.

Comparisons of the amounts of unchanged and glucuronidated compounds between hiPSC-SIECs and Caco-2 cells.

The amounts of unchanged compounds and glucuronide or sulfated metabolites were compared to raloxifene, daidzein, genistein, and bisphenol A after performing the membrane permeability assays using hiPSC-SIECs and Caco-2 cells (Table 3). The total glucuronide produced in hiPSC-SIECs was 6.4- (raloxifene) to 40- (daidzein) fold higher than that in Caco-2 cells. The total amount of unchanged compounds in basal compartments and metabolites in apical and basal compartments were 0.9- (daidzein) to 2.7- (raloxifene) folds between hiPSC-SIECs and Caco-2 cells.

Comparisons of glucuronidation rates between hiPSC-SIECs, Caco-2 cells, and hPECs using typical UGT substrates and food-derived compounds

We compared the metabolic rates of three typical UGT substrates (7-hydroxycoumarin, raloxifene, and estradiol) and three food-derived compounds (daidzein, genistein, and bisphenol A) in hiPSC-SIECs, Caco-2 cells, and hPECs (Table 4). The metabolic rates of UGT substrates were similar or slightly higher in hiPSC-SIECs (0.14–18-fold), and lower in Caco-2 cells (0.0083–0.90-fold), as compared with those in hPECs, except 7-hydroxycoumarin in Caco-2 cells (6.5-fold increase) and genistein

DMD Fast Forward. Published on October 20, 2021 as DOI: 10.1124/dmd.121.000605
This article has not been copyedited and formatted. The final version may differ from this version.

4'-glucuronide, which was neither detected in hiPSC-SIECs nor in Caco-2 cells. The metabolic rates of other known metabolites, such as 7-hydroxycoumarin sulfate and bisphenol A sulfate in hiPSC-SIECs and Caco-2 cells, were within 0.28–3.8-fold compared with those rates in hPECs.

Comparisons of mRNA expression levels for UGT isoforms between hiPSC-SIECs, Caco-2 cells, and hPECs

Figure 2 shows the results of the relative mRNA expression levels of representative UGT isoforms by real-time RT-PCR in hiPSC-SIECs and Caco-2 cells compared with hPECs. The expression levels of small intestine-specific UGT isoforms UGT1A8 and UGT1A10 in hiPSC-SIECs were within 10-fold of the levels in hPECs (1.4-fold for UGT1A8 and 0.13-fold for UGT1A10, respectively), while those in Caco-2 cells were quite low (0.027-fold for UGT1A8 and 0.0017-fold for UGT1A10, respectively). The expression levels of UGT isoforms in hiPSC-SIECs and Caco-2 cells such as UGT1A6, UGT1A9, and UGT2B7, which are not limited to the small intestinal cells, were similar to those of hPECs. The expression levels of UGT1A1 and UGT2B15 were higher in hiPSC-SIECs than in hPECs (95-fold and 127-fold for UGT1A1 and UGT2B15, respectively).

DMD Fast Forward. Published on October 20, 2021 as DOI: 10.1124/dmd.121.000605
This article has not been copyedited and formatted. The final version may differ from this version.

Discussion

When membrane permeability of hiPSC-SIECs and Caco-2 cells were compared using drugs with known intestinal availability, P_{app} values for the high-membrane permeability drugs ($P_{app} > 10 \times 10^{-6}$ cm/s) were similar between hiPSC-SIECs and Caco-2 cells. On the other hand, P_{app} differed between hiPSC-SIECs and Caco-2 cells for the low-to-medium permeability drugs ($P_{app} < 10 \times 10^{-6}$ cm/s). hiPSC-SIECs had a better correlation between P_{app} and F_a or F_aF_g than Caco-2 cells, especially with low-to-medium F_a or F_aF_g compounds. It is unclear why, but high permeability drugs are mainly passed via transcellular routes, while low-to-medium absorption compounds are passed via transcellular and paracellular routes. Since hiPSC-SIECs have lower TEER values than Caco-2 cells, it might be due to the contribution of the paracellular route, as previously discussed (Kabeya et al., 2020). Similarly, the P_{app} of food-derived compounds, including caffeic acid and gallic acid which have been reported to be passed through the paracellular route (Konishi et al., 2003; Konishi and Kobayashi, 2004), differ between hiPSC-SIECs and Caco-2 cells, supporting this explanation. Another reason might be the difference in intracellular permeability between hiPSC-SIECs and Caco-2 cells. Although total concentrations for unchanged compounds and metabolites were similar between Caco-2 cells and hiPSC-SIECs (Table 3), we could not ignore the possibility of a difference in membrane permeability between the two types of cells because we could not measure the

DMD Fast Forward. Published on October 20, 2021 as DOI: 10.1124/dmd.121.000605
This article has not been copyedited and formatted. The final version may differ from this version.

concentration of the refluxed unchanged substrates to apical compartments. Another explanation might be the involvement of intestinal transporters. Konishi et al. reported that caffeic acid is incorporated via monocarboxylic transporter 1 but gallic acid is not (Konishi et al., 2003; Konishi and Kobayashi, 2004). In our study, the fold increase in the P_{app} value of caffeic acid between hiPSC-SIECs and Caco-2 cells was higher than the fold increase of caffeic acid (5.7-fold vs. 1.7-fold), suggesting the involvement of transporter-mediated uptake as well as paracellular transport. Methotrexate is known as a substrate for both influx transporter (PCFT) and efflux transporters (MRP2, BCRP), and genistein is a substrate for efflux transporters (MRP2) (Yokooji et al., 2007, Yokooji et al., 2009, and Takaai et al., 2010, Kobayashi et al., 2013). Further studies are needed to understand the detailed mechanisms of these compounds. Based on these results, it was suggested that hiPSC-SIECs could predict the human intestinal availability better than Caco-2 cells.

When predicting the human intestinal absorption, it is important to consider not only the intestinal permeability but also metabolism in intestinal cells. For example, several compounds in food, such as daidzein and bisphenol A, are known to be metabolized by UGTs, and over 99% of these compounds were present as glucuronide metabolites in human serum (Setchell et al., 2001; Thayer et al., 2015). The P_{app} values of these compounds in hiPSC-SIECs were 4–53-fold lower than those in Caco-2 cells, suggesting the possible involvement of UGT metabolism in hiPSC-SIECs in membrane permeability

DMD Fast Forward. Published on October 20, 2021 as DOI: 10.1124/dmd.121.000605
This article has not been copyedited and formatted. The final version may differ from this version.

assays. Additionally, we observed that hiPSC-SIECs produced more glucuronidated metabolites for raloxifene, daidzein, genistein, and bisphenol A than Caco-2 cells during the membrane permeability assays. Thus, we speculated that hiPSC-SIECs might have the potential to predict human intestinal absorption of food-derived compounds via simultaneous evaluation of membrane permeability and intestinal cellular metabolism. The metabolic rates of glucuronide in hiPSC-SIECs were quantified and found to be similar or higher than those in hPECs, which were found to be much greater than in Caco-2 cells, excepting only for 7-hydroxycoumarin and bisphenol A for Caco-2 cells. Finally, to account for the differences of UGT activities, we further compared the mRNA expression levels of UGT isoforms between hiPSC-SIECs, Caco-2 cells, and hPECs. UGT mRNA expression experiments indicated the same order (hiPSC-SIECs > hPECs >> Caco-2 cells), excepting only UGT1A6 and UGT2B15 for Caco-2 cells, the expressions of which were similar between Caco-2 cells and hPECs.

7-Hydroxycoumarin is mainly glucuronidated by UGT1A6 and UGT1A9, both of which are tissue non-specific UGT isoforms (Moeller et al., 2011). Metabolic rates of 7-hydroxycoumarin are slightly higher in hiPSC-SIECs and Caco-2 cells than those in hPECs. Expression levels of UGT1A6 were also higher in hiPSC-SIECs and Caco-2 cells. This may account for differences in the metabolic rates of 7-hydroxycoumarin glucuronide in these cells. Previous reports have indicated that the UGT1A6 activity in Caco-2 cells is

DMD Fast Forward. Published on October 20, 2021 as DOI: 10.1124/dmd.121.000605
This article has not been copyedited and formatted. The final version may differ from this version.

higher than that in hPECs, consistent with our current study (Zhang et al., 2011). The metabolic rates of another metabolite, 7-hydroxycoumarin sulfate, were similar in hiPSC-SIECs and Caco-2 cells as compared with in hPECs. Therefore, we concluded that the metabolic rates of sulfate conjugate did not cause a significant impact in interpreting these results.

Raloxifene is known to have two glucuronidation sites at the 4'-OH position and 6-OH position. The 4'-OH position is conjugated by UGT1A8 and UGT1A10, which are small intestine-specific UGT isoforms, while the 6-OH position is conjugated by UGT1A1 and UGT1A8 (Kemp et al., 2002). As shown in Figure 1, P_{app} of raloxifene in hiPSC-SIECs were lower than those in Caco-2 cells. The metabolic rates of 4'-glucuronide were 0.96- and 0.014-fold in hiPSC-SIECs and Caco-2 cells, respectively, compared with those in hPECs. We also observed the expression levels of UGT1A8 and UGT1A10 were within 10-fold in hiPSC-SIECs, and far lower in Caco-2 cells compared with hPECs, which may explain the difference in metabolic rates of raloxifene 4'-glucuronide. The metabolic rates of 6-glucuronidated form were 12- and 0.030-fold in hiPSC-SIECs and Caco-2 cells as compared with hPECs. We also observed the expression levels of UGT1A1 were 119- and 0.024-fold in hiPSC-SIECs and Caco-2 cells as compared with hPECs. These results may explain the difference in metabolic rates for raloxifene 4'-glucuronide and 6-glucuronide among these three cell types.

DMD Fast Forward. Published on October 20, 2021 as DOI: 10.1124/dmd.121.000605
This article has not been copyedited and formatted. The final version may differ from this version.

β-Estradiol was determined to be a specific substrate for UGT1A1 by measuring the metabolic rate of β-estradiol 3-glucuronide (Lv et al., 2019). The metabolic rates of β-estradiol 3-glucuronide were comparable in hiPSC-SIECs (3.8-fold) and lower in Caco-2 cells (0.017-fold) as compared with that in hPECs; these results also support intestine-specific UGT activities in hiPSC-SIECs. Metabolic rates of another metabolite, β-estradiol 17-glucuronide, were similar among the three cell types. This metabolite was reported to possibly be catalyzed by UGT1A10, UGT2B7, and UGT2B17 (Asai et al., 2017).

Daidzein and genistein are also known to have two glucuronidation sites at the 4'-OH position and 7-OH position. There are some reports detailing daidzein metabolism in the intestine and the liver (Hanioka et al., 2018) showing that the 4'-glucuronidated form is mainly generated in the small intestine. The metabolic rates of these 4'-glucuronidated forms were 0.14-fold in hiPSC-SIECs and 0.0083-fold in Caco-2 cells as compared with those in hPECs. However, the metabolic rates of the 7-glucuronide were 7.1-fold in hiPSC-SIECs and 0.050-fold in Caco-2 cells as compared with those in hPECs.

Bisphenol A is known to undergo glucuronidation mainly by UGT1A9 and UGT2B15, which are abundant in the liver (Hanioka et al., 2008). These metabolic rates were 21-fold in hiPSC-SIECs and 0.5-fold in Caco-2 cells compared with hPECs. The relative mRNA expression levels of UGT2B15 were 226-fold in hiPSC-SIECs and 3.2-fold

DMD Fast Forward. Published on October 20, 2021 as DOI: 10.1124/dmd.121.000605
This article has not been copyedited and formatted. The final version may differ from this version.

in Caco-2 cells as compared with hPECs, which may explain the difference in metabolic rates of bisphenol A.

Based on these results, it was strongly suggested that the activities and expressions of intestine-specific UGT1A8 and UGT1A10 in hiPSC-SIECs were comparable with hPECs, while those in Caco-2 cells were much lower. However, it was also suggested that non-specific UGT isoforms such as UGT1A1 and UGT2B15 in hiPSC-SIECs were higher than those of hPECs. hiPSC-SIECs have great potential to predict intestinal absorption, but there are some limitations. For example, raloxifene 4'-glucuronide was reported to be present as a major metabolite in human plasma, because the intrinsic clearance of the 4'-glucuronidated form is 5.6-fold higher than the 6-glucuronidated form in intestinal microsomes (Kemp et al., 2002). We observed the metabolic rates of raloxifene 4'-glucuronide in hiPSC-SIECs were comparable to those in hPECs, but the metabolic rates of raloxifene 6-glucuronide were 12-times higher than in hPECs; thus, metabolite ratios between the 4'-glucuronide and 6-glucuronide forms were different (4'-glucuronide: 6-glucuronide ratios = 0.60 in hiPSC-SIECs and 7.9 in hPECs). Similar result was observed for daidzein. Although previous reports found that the metabolic ratio of 4'-glucuronide and 7-glucuronide in human intestinal microsomes were 1.7 (Hanioka et al., 2018), metabolite ratios between the 4'-glucuronide and 7-glucuronide forms were different (4'-glucuronide: 7-glucuronide ratios = 112 in hiPSC-SIECs and 2.2 in hPECs). We

DMD Fast Forward. Published on October 20, 2021 as DOI: 10.1124/dmd.121.000605
This article has not been copyedited and formatted. The final version may differ from this version.

therefore considered that hiPSC-SIECs reproduced glucuronic metabolism in small intestinal cells, but was not exactly the same in terms of UGT isoforms examined in this study. There are some limitations to our conclusion, because specific inhibitors for UGT isoforms are limited and the substrate specificity of UGT overlaps between each isoform (Lv et al., 2018), we could not confirm the molecular mechanisms. Further studies might be needed to confirm our speculation. We still believe that hiPSC-SIECs could be an improvement in predicting human intestinal absorption of unchanged compounds, because when considering the overall metabolic clearance rates of the unchanged compounds in this study, the metabolic clearance rates of the unchanged compounds ranged from 0.96 to 18-fold in hiPSC-SIECs and 0.017 to 6.5-fold in Caco-2 cells as compared with in hPECs. Therefore, hiPSC-SIECs might have closer characteristics to hPECs than Caco-2 cells. Further studies might improve upon these metabolic characteristics. Since we found that UGT activities and mRNA expression levels were correlated, expression of UGT isoforms could be valuable to evaluate the cellular properties of hiPSC-SIECs from individual vendors. In addition, application for human plasma concentration prediction should be conducted in combination with other *in vitro* assays such as hepatocyte metabolic stability and plasma protein binding assays, and *in silico* prediction assays.

In conclusion, this study is the first report to simultaneously compare hiPSC-SIECs, Caco-2 cells, and hPECs in terms of membrane permeability and intracellular UGT

DMD Fast Forward. Published on October 20, 2021 as DOI: 10.1124/dmd.121.000605
This article has not been copyedited and formatted. The final version may differ from this version.

metabolism. We conclude that hiPSC-SIECs might be useful for predicting the human intestinal absorption of food-derived compounds related to UGT conjugation enzymes for quantitative human risk assessment.

DMD Fast Forward. Published on October 20, 2021 as DOI: 10.1124/dmd.121.000605
This article has not been copyedited and formatted. The final version may differ from this version.

Acknowledgments

None.

Authorship Contributions

Participated in research design: Kitaguchi, Mizota, Ito, Ohno, Kobayashi, Ogawa, Qiu, Iwao, Hanioka, Tanaka, and Matsunaga

Conducted experiments: Kitaguchi, Mizota, and Ito

Performed data analysis: Kitaguchi and Ito

Wrote or contributed to the writing of the manuscript: Kitaguchi, Mizota, Ohno, Kobayashi, Iwao, Hanioka, and Matsunaga

DMD Fast Forward. Published on October 20, 2021 as DOI: 10.1124/dmd.121.000605
This article has not been copyedited and formatted. The final version may differ from this version.

References

Amidon GL, Sinko P, and Fleisher D (1988) Estimating human oral fraction dose absorbed: a correlation using rat intestinal membrane permeability for passive and carrier-mediated compounds. *Pharm Res* **5**: 651–654.

Asai Y, Sakakibara Y, Kondo M, Nadai M, and Katoh M (2017) Species and tissue differences in β-estradiol 17-glucuronidation. *Biol Pharm Bull* **40**: 1754–1758.

Gibis M (2016) Heterocyclic aromatic amines in cooked meat products: Causes, formation, occurrence, and risk assessment. *Compr Rev Food Sci Food Saf* **15**: 269–302.

Hanioka N, Naito T, and Narimatsu S (2008) Human UDP-glucuronosyltransferase isoforms involved in bisphenol A glucuronidation. *Chemosphere* **74**: 33–36.

Hanioka N, Ohkawara S, Isobe T, Ochi S, Tanaka-Kagawa T, and Jinno H (2018) Regioselective glucuronidation of daidzein in liver and intestinal microsomes of humans, monkeys, rats, and mice. *Arch Toxicol* **92**: 2809–2817.

Kabeya T, Mima S, Imakura Y, Miyashita T, Ogura I, Yamada T, Yasujima T, Yuasa H, Iwao T, and Matsunaga T (2020) Pharmacokinetic functions of human induced pluripotent stem cell-derived small intestinal epithelial cells. *Drug Metab Pharmacokinet* **35**: 374–382.

Kemp DC, Fan PW, and Stevens JC (2002) Characterization of raloxifene glucuronidation *in vitro*: contribution of intestinal metabolism to presystemic clearance. *Drug Metab*

Dispos **30**: 694–700.

Kobayashi S, Shinohara M, Nagai T, and Konishi Y (2013) Transport mechanisms for soy isoflavones and microbial metabolites dihydrogenistein and dihydrodaidzein across monolayers and membranes. *Biosci Biotechnol Biochem* **77**: 2210–2217.

Konishi Y and Kobayashi S (2004) Transepithelial transport of chlorogenic acid, caffeic acid, and their colonic metabolites in intestinal Caco-2 cell monolayers. *J Agric Food Chem* **52**: 2518–2526.

Konishi Y, Kobayashi S, and Shimizu M (2003) Transepithelial transport of *p*-coumaric acid and gallic acid in Caco-2 cell monolayers. *Biosci Biotechnol Biochem* **67**: 2317–2324.

Larregieu CA and Benet LZ (2013) Drug discovery and regulatory considerations for improving *in silico* and *in vitro* predictions that use Caco-2 as a surrogate for human intestinal permeability measurements. *AAPS J* **15**: 483–497.

Livak KJ and Schmittgen TD (2001) Analysis of relative gene expression data using real-time quantitative PCR and the $2^{-\Delta\Delta CT}$ method. *Methods* **25**: 402–408.

Luca SV, Macovei I, Bujor A, Miron A, Skalicka-Woźniak K, Aprotosoaie AC, and Trifan A (2020) Bioactivity of dietary polyphenols: The role of metabolites. *Crit Rev Food Sci Nutr* **60**: 626–659.

Lv X, Zhang JB, Hou J, Dou TY, Ge GB, Hu WZ, and Yang L (2019) Chemical probes for

human UDP-glucuronosyltransferases: A comprehensive review. *Biotechnol J* **14**: e1800002.

Lv X, Xi Y, Finel M, Wu J, Ge G, and Yang L (2019) Recent progress and challenges in screening and characterization of UGT1A1 inhibitors. *Acta Pharm Sin B* **9**: 258–278.

Michiba K, Maeda K, Kurimori K, Enomoto T, Shimomura O, Takeuchi T, Nishiyama H, Oda T, and Kusuhara H (2021) Characterization of the human intestinal drug transport with Ussing chamber system incorporating freshly isolated human jejunum. *Drug Metab Dispos* **49**: 84–93.

Moeller TA, Rose T, and Heyward S (2011) Determination of 7-hydroxycoumarin specificity using recombinant human enzymes of uridine 5'-diphospho-glucuronosyltransferase (UGT). *17th North American Regional ISSX Meeting* P-31.

Negoro R, Takayama K, Kawai K, Harada K, Sakurai F, Hirata K, and Mizuguchi H (2018) Efficient generation of small intestinal epithelial-like cells from human iPSCs for drug absorption and metabolism studies. *Stem Cell Rep* **11**: 1539–1550.

Nishimuta H, Sato K, Yabuki M, and Komuro S (2011) Prediction of the intestinal first-pass metabolism of CYP3A and UGT substrates in humans from *in vitro* data. *Drug Metab Pharmacokinet* **26**: 592–601.

Ohno S and Nakajin S (2009) Determination of mRNA expression of human

UDP-glucuronosyltransferases and application for localization in various human tissues by real-time reverse transcriptase-polymerase chain reaction. *Drug Metab Dispos* **37**: 32–40.

Punt A, Peijnenburg AACM, Hoogenboom RLAP, and Bouwmeester H (2017) Non-animal approaches for toxicokinetics in risk evaluations of food chemicals. *ALTEX* **34**: 501–514.

Setchell KDR, Brown NM, Desai P, Zimmer-Nechemias L, Wolfe BE, Brashear WT, Kirschner AS, Cassidy A, and Heubi JE (2001) Bioavailability of nutrients and other bioactive components from dietary supplements bioavailability of pure isoflavones in healthy humans and analysis of commercial soy isoflavone supplements. *J Nutr* **131**: 1362S–1375S.

Shimizu M (2011) Modulation of intestinal functions by dietary substances: An effective approach to health promotion digestion and absorption functions of the gut and functional foods. *J Tradit Complement Med* **2**: 81–83.

Takaai M, Sakata J, Ishida K, Taguchi M, and Hashimoto Y (2010) Mechanisms for transport of methotrexate across apical and basolateral membranes in human intestinal epithelial Caco-2 cells. *Jpn J Pharm Health Care Sci* **36**: 63–71.

Takenaka T, Harada N, Kuze J, Chiba M, Iwao T, and Matsunaga T (2016) Application of a human intestinal epithelial cell monolayer to the prediction of oral drug absorption in

humans as a superior alternative to the Caco-2 cell monolayer. *J Pharm. Sci* **105**: 915–924.

Thayer KA, Doerge DR, Hunt D, Schurman SH, Twaddle NC, Churchwell MI, Garantziotis S, Kissling GE, Easterling MR, Bucher JR, and Birnbaum LS (2015) Pharmacokinetics of bisphenol A in humans following a single oral administration. *Environ Int* **83**: 107–115.

Thompson LA and Darwish WS (2019) Environmental chemical contaminants in food: Review of a global problem. *J Toxicol* **2019**: 2345283.

Vancamelbeke M and Vermeire S (2017) The intestinal barrier: A fundamental role in health and disease. *Expert Rev Gastroenterol Hepatol* **11**: 821–834.

Wu B, Kulkarni K, Basu S, Zhang S, and Hu M (2011) First-pass metabolism via UDP-glucuronosyltransferase: A barrier to oral bioavailability of phenolics. *J Pharm Sci* **100**: 3655–3681.

Yokooji T, Yumoto R, Nagai J, Takano M, Yokooji T, and Murakami T (2007) Role of intestinal efflux transporters in the intestinal absorption of methotrexate in rats. *J Pharm Pharmacol* **59**: 1263–1270.

Yokooji T, Mori N, and Murakami T (2009) Site-specific contribution of proton-coupled folate transporter/haem carrier protein 1 in the intestinal absorption of methotrexate in rats. *J Pharm Pharmacol* **61**: 911–918.

Yoshida S, Honjo T, Iino K, Ishibe R, Leo S, Shimada T, Watanabe T, Ishikawa M, Maeda K, Kusuhara H, Shiraki N, and Kume S (2021) Generation of human-induced pluripotent stem cell-derived functional enterocyte-like cells for pharmacokinetic studies. *Stem Cell Rep* **16**: 295–308.

Zhang H, Tolonen A, Rousu T, Hirvonen J, and Finel M (2011) Effects of cell differentiation and assay conditions on the UDP-glucuronosyltransferase activity in Caco-2 cells. *Drug Metab Dispos* **39**: 456–464.

Footnotes

Financial Disclosure: This work received no external funding.

Declaration of interest: The authors report no conflicts of interest.

The intellectual property rights are included with the price of commercial hiPSC-SIECs.

DMD Fast Forward. Published on October 20, 2021 as DOI: 10.1124/dmd.121.000605
This article has not been copyedited and formatted. The final version may differ from this version.

Figure Legends

Fig. 1. Relationship between apparent permeability coefficients (P_{app}) and intestinal availability (F_a or F_aF_g) for 21 drugs. (A) Human induced pluripotent stem cell-derived small intestinal epithelial cells (hiPSC-SIECs) or (B) Caco-2 cells were incubated with transport buffer containing each of the 21 different drugs for 90 min at 37°C. The regression curves between the P_{app} and F_a or F_aF_g of these 21 drugs were fitted to the following formula in accordance with previous reports (Takenaka et al., 2016 and Amidon et al., 1988): F_a or $F_aF_g = 1\text{-}e^{-Psf \times Papp}$. Compounds used were as follows: 1, Piroxicam; 2, Carbamazepine; 3, Verapamil; 4, Warfarin; 5, Antipyrine; 6, Cephalexin; 7, Metoprolol; 8, Propranolol; 9, Acebutolol; 10, Ribavirin; 11, Metformin; 12, Hydrochlorothiazide; 13, Terbutaline; 14, Cimetidine; 15, Enalapril; 16, Ranitidine; 17, Atenolol; 18, Sulpiride; 19, Pravastatin; 20, Methotrexate; and 21, Raloxifene. Data are presented as mean for hiPSC-SIECs (n = 2) and mean ± standard deviation for Caco-2 cells (n = 3).

Fig. 2. Relative expression levels of genes encoding UDP-glucuronosyltransferase (UGT) isoforms of human induced pluripotent stem cell-derived small intestinal epithelial cells (hiPSC-SIECs) and Caco-2 cells. Real-time reverse transcription polymerase chain reaction analysis of the expression levels of UGT isoform-related

DMD Fast Forward. Published on October 20, 2021 as DOI: 10.1124/dmd.121.000605
This article has not been copyedited and formatted. The final version may differ from this version.

proteins. mRNA levels were normalized to those of GAPDH mRNA gene expression levels in the human primary enterocytes (hPECs), the levels of which were arbitrarily defined as 100. The gene expression levels of hPECs were measured in and averaged across two separate lots. Data are presented as mean ± standard deviation (n = 3) for hiPSC-SIECs and Caco-2 cells.

Table 1. Primer sequences used for real-time polymerase chain reaction analysis.

Gene name	F primer	R primer
UGT1A1	5′-AATAAAAAAGGACTCTGCTATGCT-3′	5′-ACATCAAAGCTGCTTTCTGC-3′
UGT1A6	5′-CATGATTGTTATTGGCCTGTAC-3′	5′-TCTGTGAAAAGAGCATCAAACT-3′
UGT1A8	5′-GAAAGCACAAGTACGAAGTTTG-3′	5′-GGGAGGGAGAAATATTTGGC-3′
UGT1A9	5′-TGGAAAGCACAAGTACGAAGTATATA-3′	5′-GGGAGGGAGAAATATTTGGC-3′
UGT1A10	5′-GAAAGCACAGGCACAAAGTATA-3′	5′-GGGAGGGAGAAATATTTAGCAAC-3′
UGT2B7	5′-GGAGAATTTCATCATGCAACAGA-3′	5′-CAGAACTTTCTAGTTATGTCACCAAATATTG-3′
UGT2B15	5′-CTTCTGAAAATTCTCGATAGATGGAT-3′	5′-CATCTTTACAGAGCTTGTTACTGTAGTCAT-3′
GAPDH	5′-TCCACTGGCGTCTTCACC-3′	5′-GGCAGAGATGATGACCCTTTT-3′

DMD Fast Forward. Published on October 20, 2021 as DOI: 10.1124/dmd.121.000605
This article has not been copyedited and formatted. The final version may differ from this version.

Table 2. P_{app} of food-derived compounds in human induced pluripotent stem cell-derived small intestinal epithelial cells (hiPSC-SIECs) and Caco-2 cells.

Compound	P_{app} (10^{-6} cm/s)	
	hiPSC-SIECs	Caco-2 cells
Daidzein	1.6	36.8 ± 1.6
Genistein	2.7	33.7 ± 1.0
Quercetin	0.46	9.49 ± 0.64
Curcumin	0.07	3.50 ± 0.81
Epicatechin	0.13	0.12 ± 0.08
Epigallocatechin	0.34	0.29 ± 0.06
Epigallocatechin gallate	0.16	0.12 ± 0.03
Caffeic acid	1.03	0.18 ± 0.05
Gallic acid	0.41	0.24 ± 0.05
Bisphenol A	4.3	29.7 ± 2.2
Bisphenol S	5.9	23.4 ± 0.7
MeIQx	1.36	7.59 ± 0.15
Acrylamide	23.3	32.3 ± 0.8
Fenitrothion	34.0	25.4 ± 1.3
Picloram	3.88	2.98 ± 0.15

The cells were incubated with transport buffer containing each of the food-derived compounds at 37℃ for 90 min. The solution was collected from the basal chambers at every 30 min. Unchanged substrates were measured using ultraperformance liquid chromatography-tandem mass spectrometry. Data are presented as the mean for hiPSC-SIECs (n = 2) and mean ± standard deviation for Caco-2 cells (n = 3).

DMD Fast Forward. Published on October 20, 2021 as DOI: 10.1124/dmd.121.000605
This article has not been copyedited and formatted. The final version may differ from this version.

Table 3. The amounts of unchanged compounds and metabolites after the membrane permeability assays in human induced pluripotent stem cell-derived small intestinal epithelial cells (hiPSC-SIECs) and Caco-2 cells.

		Amounts (pmol/1.5 h)	
Compounds		hiPSC-SIECs	Caco-2 cells
Raloxifene	Unchanged (Basal)	2.6	38.2 ± 5.2
	Glucuronide (Apical)	27.0	7.3 ± 0.5
	Glucuronide (Basal)	68.6	7.5 ± 0.4
Daidzein	Unchanged (Basal)	49	504 ± 31
	Glucuronide (Apical)	238	8.3 ± 0.6
	Glucuronide (Basal)	202	2.8 ± 0.1
Genistein	Unchanged (Basal)	167	450 ± 14
	Glucuronide (Apical)	221	23.7 ± 1.3
	Glucuronide (Basal)	158	3.5 ± 0.2
Bisphenol A	Unchanged (Basal)	111	325 ± 48
	Glucuronide (Apical)	65.1	16.4 ± 2.0
	Glucuronide (Basal)	879	26.4 ± 3.5
	Sulfate (Apical)	77.0	53.7 ± 2.5
	Sulfate (Basal)	21.7	10.2 ± 1.1

The cells were incubated with transport buffer containing each of the food-derived compounds at 37℃ for 90 min. Unchanged substrates and metabolites were measured using ultraperformance liquid chromatography-tandem mass spectrometry. Data are presented as the mean for hiPSC-SIECs (n = 2) and mean ± standard deviation for Caco-2 cells (n = 3).

DMD Fast Forward. Published on October 20, 2021 as DOI: 10.1124/dmd.121.000605
This article has not been copyedited and formatted. The final version may differ from this version.

Table 4. Comparison of metabolic rates of typical UDP-glucuronosyltransferase (UGT) substrates and food-derived compounds between human induced pluripotent stem cell-derived small intestinal epithelial cells (hiPSC-SIECs), Caco-2 cells, and human primary enterocytes (hPECs).

Compound	Metabolite	Metabolic rate (pmol/2 h/mg protein)		
		hiPSC-SIECs	Caco-2 cells	hPECs
7-Hydroxycoumarin	glucuronide	47.2	39.9 ± 1.7	6.10
	sulfate	19.6	4.90 ± 0.40	5.10
Raloxifene	4′-glucuronide	6.33	0.09 ± 0.01	6.63
	6-glucuronide	10.5	0.025 ± 0.001	0.843
Estradiol	3-glucuronide	5.98	0.027 ± 0.005	1.59
	17-glucuronide	0.054	0.063 ± 0.015	0.070
Daidzein	7-glucuronide	60.1	0.43 ± 0.05	8.4
	4′-glucuronide	0.54	0.032 ± 0.003	3.86
Genistein	7-glucuronide	15.5	0.69 ± 0.02	5.8
	4′-glucuronide	N.D.	N.D.	0.99
Bisphenol A	glucuronide	27.7	0.70 ± 0.03	1.57
	sulfate	6.10	1.69 ± 0.18	6.08

These cells were incubated with the apical and basal transport buffer for hiPSC-SIECs and Caco-2 cells or incubation medium for hPECs containing 10 μM UGT substrates or food-derived compounds for 120 min at 37℃. Supernatants were collected, and metabolites were measured using ultraperformance liquid chromatography-tandem mass spectrometry. The metabolic rates of hPECs were measured in and averaged across two separate lots. Data are presented as mean for hiPSC-SIECs (n = 2) and mean ± standard deviation for Caco-2 cells (n = 3). N.D.: Not detected.

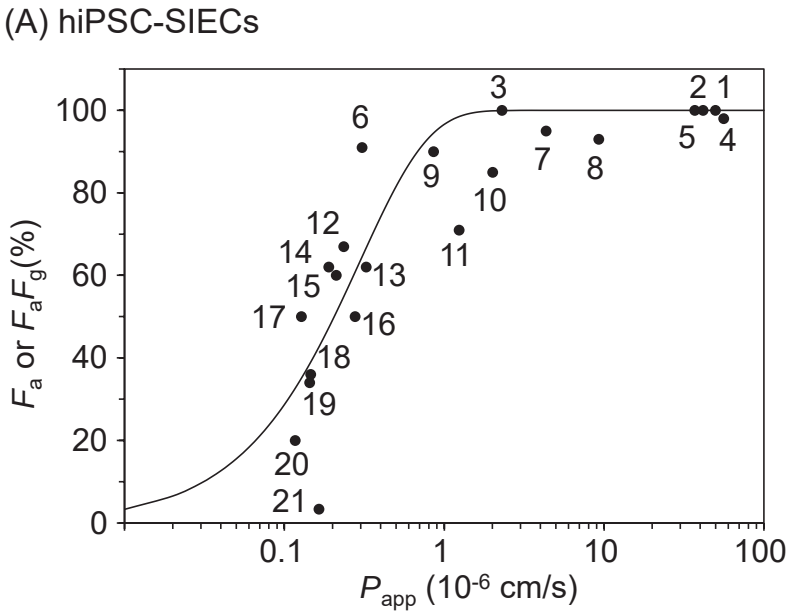

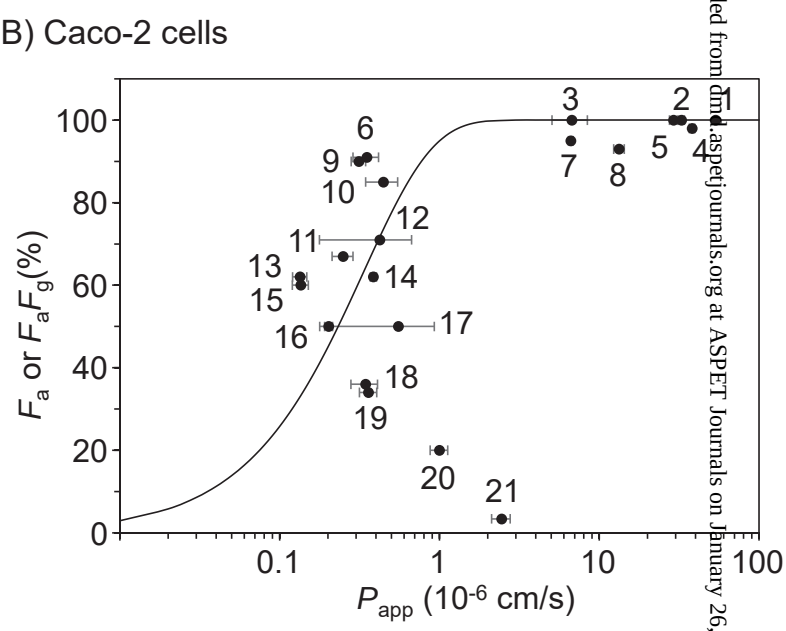

Figure 1

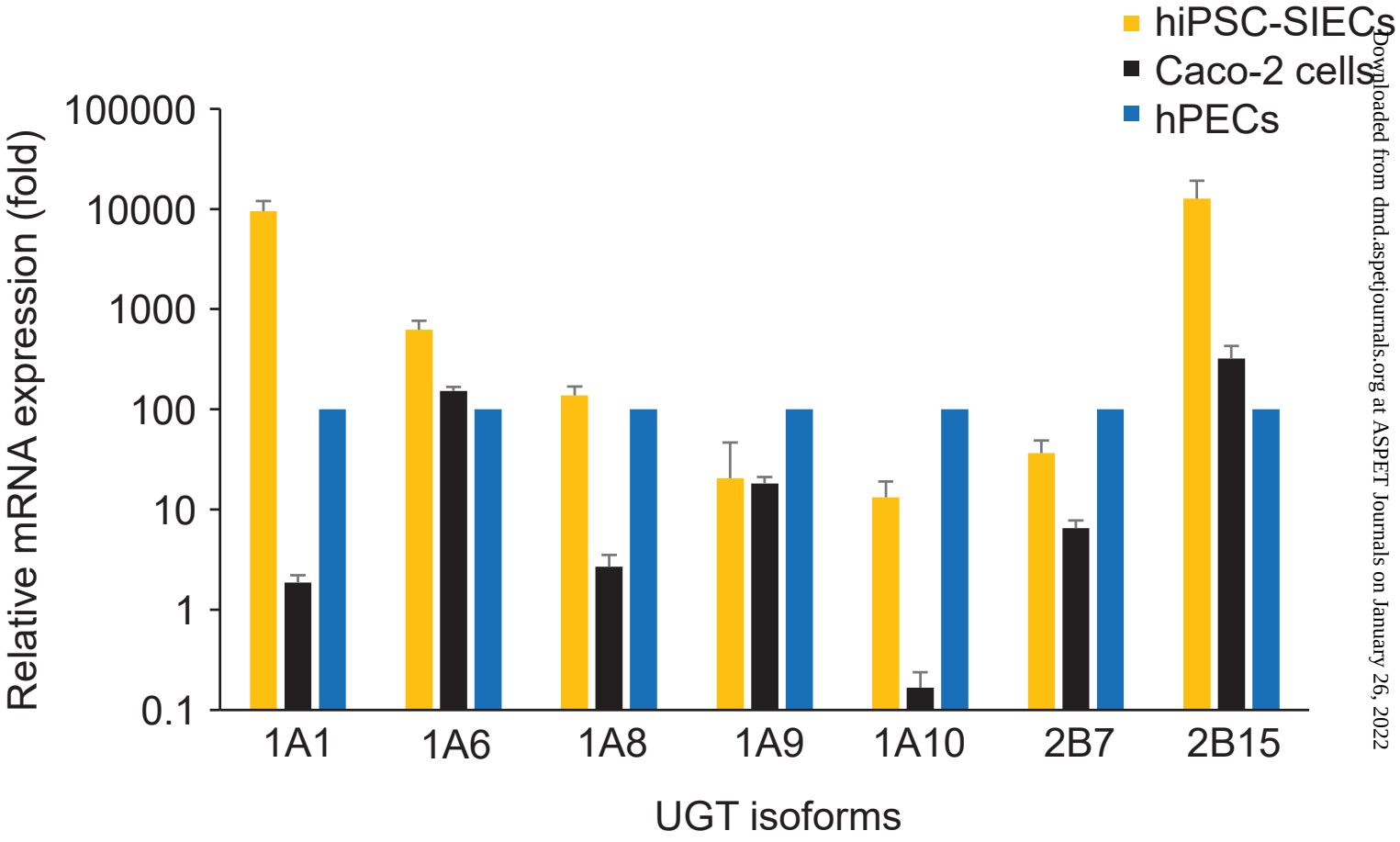

Figure 2

Simultaneous evaluation of membrane permeability and UDP-glucuronosyltransferase-mediated metabolism of food-derived compounds using human induced pluripotent stem cell-derived small intestinal epithelial cells

Takashi Kitaguchi [a, *], Taisei Mizota [a], Mina Ito [a], Katsutoshi Ohno [a], Kazuhiro Kobayashi [a], Isamu Ogawa [b], Shimeng Qiu [b], Takahiro Iwao [b], Nobumitsu Hanioka [c], Mitsuru Tanaka [a], and Tamihide Matsunaga [b]

[a] Global Food Safety Institute, Nissin Foods Holdings Co., Ltd., 2100 Tobuki-machi, Hachioji, Tokyo, 192-0001, Japan

[b] Department of Clinical Pharmacy, Graduate School of Pharmaceutical Sciences, Nagoya City University, 3-1 Tanabe-dori, Mizuho-ku, Nagoya, 467-8603, Japan

[c] Department of Health Pharmacy, Yokohama University of Pharmacy, 601 Matano-cho, Totsuka-ku, Yokohama, 245-0066, Japan

Supplemental Table 1. Pathway and transporter susceptibility during intestinal absorption and reported F_a or F_aF_g values in humans of 21 tested drugs.

No.	Drugs	Pathway for absorption/transporter/metabolic susceptibility	F_a or F_aF_g (%)	References
1	Piroxicam	Not reported	100	1)
2	Carbamazepine	Transcellular	100	2)
3	Verapamil	Transcellular/CYP3A4	100	2)
4	Warfarin	Transcellular	98	2)
5	Antipyrine	Not reported	100	3)
6	Cephalexin	Transcellular/PEPT1	91	3)
7	Metoprolol	Transcellular	95	2)
8	Propranolol	Transcellular	93	2)
9	Acebutolol	Transcellular/P-gp	90	4)
10	Ribavirin	Nucleoside transporters	85	5)
11	Metformin	Paracellular	71	2)
12	Hydrochlorothiazide	Paracellular	67	2)
13	Terbutaline	Paracellular	62	4)
14	Cimetidine	Paracellular/P-gp, BCRP	62	2)
15	Enalapril	Not reported	60	6)
16	Ranitidine	Paracellular/P-gp	50	2)
17	Atenolol	Paracellular	50	2)
18	Sulpiride	Paracellular	36	7)
19	Pravastatin	Paracellular/OATP2B1	34	2)
20	Methotrexate	Transcellular/PCFT, BCRP,	20	2)

		MRP2		
21	Raloxifene	UGT	3.4	8)

References for Supplemental Table 1

1) Shohin IE, Kulinich JI, Ramenskaya GV, Abrahamsson B, Kopp S, Langguth P, Polli JE, Shah VP, Groot DW, Barends DM, and Dressman JB (2014) Biowaiver monographs for immediate release solid oral dosage forms: piroxicam. *J Pharm Sci* **103**: 367–377.
2) Skolnik S, Lin X, Wang J, Chen XH, He T, and Zhang B (2010) Towards prediction of *in vivo* intestinal absorption using a 96-well Caco-2 assay. *J Pharm Sci* **99**: 3246–3265.
3) Varma MVS, Obach RS, Rotter C, Miller HR, Chang G, Steyn SJ, El-Kattan A, and Troutman MD (2010) Physicochemical space for optimum oral bioavailability: contribution of human intestinal absorption and first-pass elimination. *J Med Chem* **53**: 1098–1108.
4) Sugano K, Takata N, Machida M, Saitoh K, and Terada K (2002) Prediction of passive intestinal absorption using bio-mimetic artificial membrane permeation assay and the paracellular pathway model. *Int J Pharm* **241**: 241–251.
5) Dixit NM and Perelson AS (2006) The metabolism, pharmacokinetics and mechanisms of antiviral activity of ribavirin against hepatitis C virus. *Cell Mol Life Sci* **63**: 832–842.
6) Kabeya T, Mima S, Imakura Y, Miyashita T, Ogura I, Yamada T, Yasujima T, Yuasa H, Iwao T, and Matsunaga T (2020) Pharmacokinetic functions of human induced pluripotent stem cell-derived small intestinal epithelial cells. Drug Metab Pharmacokinet 35: 374–382.
7) Tavelin S, Taipalensuu J, Soderberg L, Morrison R, Chong S, and Artursson P (2003) Prediction of the oral absorption of low-permeability drugs using small intestine-like 2/4/A1 cell monolayers. *Pharm Res* **20**: 397–405.
8) Mizuma T (2009) Intestinal glucuronidation metabolism may have a greater impact on

oral bioavailability than hepatic glucuronidation metabolism in humans: a study with raloxifene, substrate for UGT1A1, 1A8, 1A9, and 1A10. *Int J Pharm* **378**: 140–141.